Proceedings of the 10th World Congress on Momentum, Heat and Mass Transfer (MHMT 2025)
Barcelona, Spain - April, 2025
Paper No. ENFHT 171
DOI: 10.11159/enfht25.171

Heat Transfer Enhancement by Jet Impingement on The Pin-Fins Channel Flow

R. X. Feng[1], T. L. Dong[1], L. W. Li[1], W. Li[1], W. T. Ji[2], J. M. Wu[1*]
[1]State Key Laboratory for Strength and Vibration of Mechanical Structures
Shaanxi Key Laboratory of Environment and Control for Flight Vehicle
School of Aerospace, Xi'an Jiaotong University
Xi'an, Shaanxi, China
fengrx@stu.xjtu.edu.cn; dtl991108@stu.xjtu.edu.cn; charlotte384@stu.xjtu.edu.cn; waylee@xjtu.edu.cn
wjmxjtu@xjtu.edu.cn*
[2]Key Laboratory of Thermo-Fluid Science and Engineering of MOE
School of Energy and Power Engineering, Xi'an Jiaotong University
Xi'an, Shaanxi, China
wentaoji@xjtu.edu.cn

***Abstract*:** Pin-fin arrays and jets play an important role in turbine blade cooling. In order to investigate the effect of jet impingement on the heat transfer enhancement of the pin-fins channel, computational models of rectangular channels with 1, 2, 3 or 4 rows of staggered pin-fins have been designed. The flow and heat transfer characteristics of the models are numerically investigated. The numerical results between conditions of jet flow generated by a perforated plate in front of the pin-fins arrays and uniform incoming flow are compared. The effect of jet holes arrangements on the perforated plate is also checked. The numerical results reveal that under jet conditions, the Nusselt number for the heated wall under the first two rows of pin-fins is 2-3 times larger than under uniform flow, but the friction factor of the channel is 100 times larger because of too small cross sectional area ratio of jet holes to the rectangular channel. The area ratio is an important factor affecting the heat transfer of the pin-fins channel and will be explored further. Staggered arrangement of jet holes shifts the heat transfer enhancement zone backward, showing stronger heat transfer in the rear pin-fin region.

***Keywords*:** Jet impingement; Pin-fins; Perforated plate; Heat transfer; Flow resistance

1. Introduction

Gas turbine is the core power equipment of energy efficient conversion and clean utilization system [1]widely used in aviation propulsion, ship propulsion, ground power generation and other fields. However, the trailing edge of turbine blade is subjected to high temperature, poor heat transfer and strength because of the narrow hollow space and complex external high temperature gas flow. Therefore, the enhancement of blade trailing edge cooling efficiency is very important with the increase of the turbine inlet temperature in development of the modern gas turbine system with higher efficiency and power.

Nowadays, pin-fin cooling has been widely used in the trailing edge of turbine blades in the existing gas turbine equipment, which can improve the heat transfer of trailing edge and enhance the strength of structure as well. There already have been many studies on the influencing factors of pin-fins channel cooling. Vanfossen et al.[2] found that short pin-fins can enhance the heat transfer of the channel flow significantly in comparison with that of a plain channel with no pin-fins. The effect of the cross-sectional shape and arrangement of the pin-fins on the heat transfer characteristics has been extensively explored in studies [3-7]. The results show that the heat transfer performance of drop-shaped pin-fins, elliptical pin-fins and triangular pin-fins are better than that of circular pin-fins. Axtmann et al.[8] concluded that the channels with short pin-fins (H/D = 2) had better heat transfer than those with long pin-fins (H/D = 4). For these studies, the incoming flow in front of the fin-fins arrays is generally uniform.

In recent years, cooling strategy utilizing high velocity jets impinging for the trailing edge cooling of turbine blades was proposed and investigated. The jet is usually formed by a perforated plate positioned in the channel. Ahn et al.[9], Chung et al.[10], Lau et al.[11] and Shin et al.[12] investigated the different effects of the shape and arrangement of the holes in the perforated plate on the heat transfer of plain channel flow. The results demonstrate that the elongated holes have the best heat transfer among all hole shapes for the same area ratio of the blockage, and the inclined hole arrays

also significantly improves the heat transfer of the channel flow.

From above literatures, both of pin-fins and jet exhibit excellent cooling characteristics in the channel flow. It can be expected that the composite cooling based on these two cooling structures could achieve better cooling effect for the blade trailing edge. So far, a few studies have been carried out on the cooling characteristics of the new composite cooling structure. Schekman et al.[13] investigated the local heat transfer near a single short pin-fin under jet impingement, and found that the intensity of the heat transfer was related to the distance of the pin-fin from the jet outlet. In Kan et al.[14]'s experimental and numerical study, it is found that under jet flow, the *Nu* on the heated wall around the first two rows of pin-fins is 2-3 times higher than that of the uniform flow, and the area of the jet orifice has a significant effect on the heat transfer and friction losses. Motivated by these positive results, the present study focuses on the heat transfer enhancement by jet impingement on pin-fins channel. A total of 13 sets of computational models have been designed and numerically investigated on the effects of flow conditions and jet hole arrangements on the flow and heat transfer characteristics of pin-fins channel.

2. Computational models

The 13 sets of computational models designed in this paper are shown in Table 1. Case1 is established according to the experimental model from literature [13] shown in Fig. 1, to validate the reliability of the numerical models and methods used in the present study. So the geometrical sizes of case1 is completely taken from the test section in literature [13], where the origin is at the centre of the pin-fin base. The cases 2-5 are the computational models to simulate the traditional rectangular channel flow with 1, 2, 3 or 4 rows of staggered pin-fins under uniform inlet condition as baseline for comparison. Cases 6-9 are the computational models not only having the same arrangement of pin-fins array as cases2-5 respectively, but also having a perforated plate with round jet holes positioned in front of the first row of pin-fins exactly to investigate the effect jet impingement on the pin-fins channel flow. To further study the effect of jet hole arrangement on the flow and heat transfer of pin-fins channel, cases10-13 are designed based on the Case9 with four rows of pin-fins shown in Fig. 2, but with different jet hole arrangement on the perforated plate shown in Fig. 3. Table 1 gives some details about cases 1-13.

Table 1 Computational models for Case1-13

Model to to validate the reliability					
Case1		With single jet pipe and single pin-fin in [13]			
Models with different rows of pin-fins arrays					
Uniform flow		**Jet flow (Formed by a perforated plate)**			
Case2	1 row	**Case6**	1 row		
Case3	2 rows	**Case7**	2 rows		
Case4	3 rows	**Case8**	3 rows		
Case5	4 rows	**Case9**	4 rows		
Models with different configurations of perforated plate under four rows of pin-fins					
	D_j/mm	**Jet hole position relative to first row of pin-fins**	**Jet holes layer**	**Tilt angle of jet hole axis to heated wall**	**Area ratio**
Case9	3	Aligned	1	0	3.93%
Case10	2	Aligned	1	0	1.75%
Case11	3.29	Staggered	1	0	3.93%
Case12	2.12	Aligned	2	0	3.92%
Case13	2.12	Aligned	2	10°	3.92%

The sizes of channel and pin-fins are the same for cases 2-13. The origin is located on the bottom surface, midway behind the perforated blockage. As shown in Fig. 2, channel has a length L = 0.695 m, height H = 0.015 m, and width W = 0.072 m. The pin-fin diameter (D) is 0.006 m, the aspect ratio (H/D) of pin-fin is 2.5. The streamwise distance (X) and spanwise distance (S) between pin-fins are both 2 times the diameter of pin-fin according to literature [14]. The diameter (D_j) of jet holes in Case9 equals to 0.003 m. The first row of pin-fins arrays are located 0.006 m downstream of the perforated plate to ensure the impact effect was large enough according to literature [13]. The top and bottom walls of the test zone were heated by constant heat flux. The inlet and outlet sections of the calculation model were extended to ensure the incoming flow in front of the perforated plate develops fully, and to reduce the possible backflow

at the outlet on the test zone [15]. In order to reduce the calculation workload, the actual computational model is only half because of the symmetry in the channel width direction. The jet holes diameters for the cases10-13 are 2 mm, 3.29 mm, 2.12 mm and 2.12 mm, thus the cross-section area ratios of jet holes to the channel are as shown in Table 1.

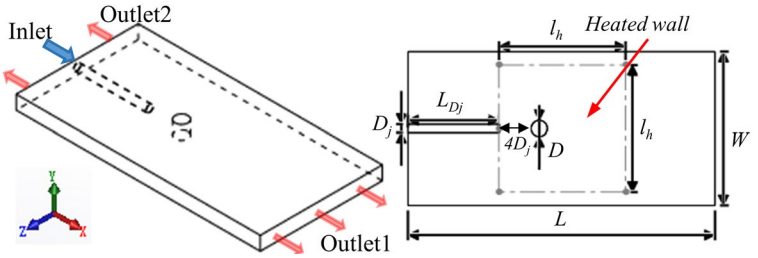

Fig. 1 Computational model of rectangular channel with single jet pipe and single pin-fin

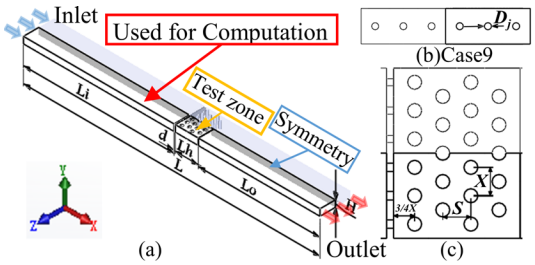

Fig. 2 Computational model for Case9

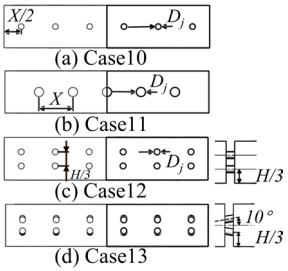

Fig. 3 Perforated plates for Case10-13

3. Numerical methods and some details

3.1. Governing equations and boundary conditions

In this paper, steady state simulations are carried out with air as coolant in turbulent regime. The air is taken as ideal gas to consider the change of density with pressure because of the high velocity jet flow. The other thermophysical properties of air are taken as constant at normal temperature because the change of air temperature is small in the computational domain. The turbulent flow governing equations of airflow can be referred in Jin et al.[7]. The coupled heat transfer calculation is carried out by considering the heat conductivity in pin-fins. The definitions of the dimensional parameters and nondimensional numbers used in the present paper, and the post-processing methods of numerical results are the same as in literature [15].

As stated above, the reliability of the numerical models and method are validated by comparing the numerical results with experiment results in literature [13], based on the computational model of Fig. 1. Thus the boundary conditions of Fig. 1 are determined based on the test conditions described in literature [13], with the Reynolds number of the jet pipe (Re_{Dj}) being 17500. While for Fig. 2, the inlet condition is a mass-flow-inlet with a fixed temperature T=295.15 K for cases 2-13. The outlet condition of channel is pressure outlet. The top and bottom walls of the test zone are heated by constant heat flux and the computational domain has a symmetry plane. The material of pin-fins is PMMA. Fluid-solid interface is set up at the interface between the fluid and solid domains, the others walls are adiabatic and non-slip boundaries. It should be noted that for the simulation of cases 2-13, Re_{Dh} is the Reynolds number of the rectangular channel and is used to determine the inlet mass flow rate.

3.2. Meshing and grid independence analysis

In this paper, ANSYS ICEM CFD 2020 R2 software is used to generate the structural mesh in the fluid and solid domains. The boundary layer grids are drawn around the pin-fins and near all the channel walls, and the first grid height of the boundary layer was set small enough to meet the criterion that the y+ value is close to 1. The grid independence analysis for both computational models of Fig. 1 and Fig. 2 is carried out as shown in Fig. 4. A grid system of 1.33 million for the model of Fig. 1 and 3.2 million for model of Fig. 2 is chosen to obtain the following grid independent numerical results.

3.3. Validation of numerical simulation methods

In order to verify the feasibility of the numerical simulation method as well as to select an appropriate turbulence model, a total of four turbulence models are used in this paper to simulate the computational model of Fig. 1. The numerical results of local Nusselt number using the four turbulence models are compared to the experimental results of literature [13] as shown in Fig. 5. It is found that the numerical results based on RNG k-ε turbulence model are better agreements with the experimental results than others, except in the vicinity of x/D = -0.5 where is near the leading edge of the pin-fin in Fig. 1. Therefore, the RNG k-ε is used as the turbulence model for the simulation cases 2-13.

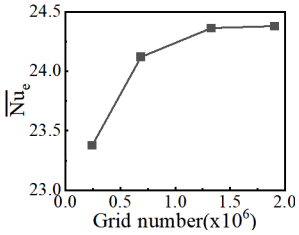

(a) Case1

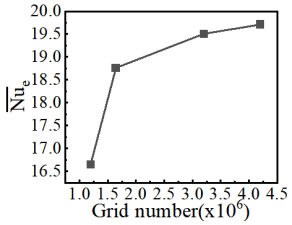

(b) Case9

Fig. 4 Averaged Nusselt number on the heated wall

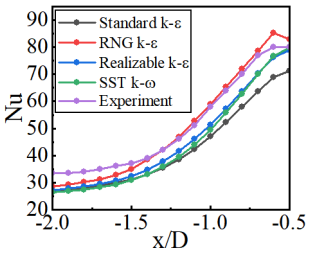

Fig. 5 *Nu* in the plane of symmetry for l/D_j = 4.0

4. Results and discussion

4.1. Effect of jet impingement on the flow and heat transfer in channels with different rows of pin-fins

In this section, the results of cases 2-9 are presented and compared to understand the effect of the jet impingement on the flow and heat transfer in the channels with 1-4 rows of pin-fins.

Flow field

As we know, under uniform inlet flow condition, air flowing around the pin-fins always forms horseshoe vortices and wake vortices. To save space, only the flow structure of Case5 is shown in Fig. 6 and Fig. 7. But for cases 6-9 under high velocity jet flow formed by the perforated plate, the flow structure around the pin-fins becomes much more complex. As shown in Fig. 6(b)(c)(d) for Case6, 7 and 9, a ring of high-velocity zones is formed around the 1st row of pin-fins by the jet impinging, and the flow separation on the pin-fins surface moves backward. The wake zones behind the 1st row of pin-fins are greatly reduced and obviously deflected due to the 2nd row of pin-fins. Meanwhile, a negative pressure zone is formed between the perforated plate and the first row of pin-fins, causing the air reverse flow. The secondary impact flow to the heated wall after the jet impingement on pin-fins surface can be observed in Fig. 7(b), which greatly increases the near wall velocity in the zone between the 1st-2nd row of pin-fins as shown in Fig. 6(f)-(h).

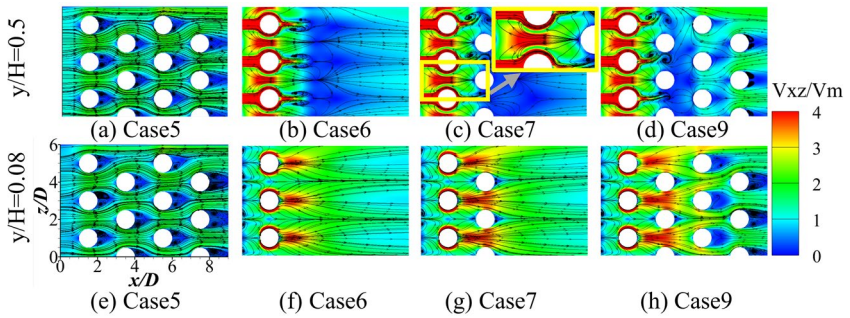

(a) Case5 (b) Case6 (c) Case7 (d) Case9

(e) Case5 (f) Case6 (g) Case7 (h) Case9

Fig. 6 Flow structure at different *xz*-plane, Re_{Dh}=6000

By comparing Fig. 6 (b)-(d) and (f)-(h), one can find the jet impingement has an important effect on the flow around the 1st row of pin-fins. The 2nd row of pin-fins has a converging and accelerating effect on the boundary layer flow near the heated wall, thereby expanding the high-velocity zone, as shown in Fig. 6(f) and (g). For the Case8, the jet impingement effect on the 3rd row of pin-fins is decreased but with a pair of large transverse vortices generated at the leading edge of the 3rd row of pin-fins, as shown in Fig. 7(c). More fluid is rectified by the 3rd row of pin-fins and the flow becomes more uniform. For the Case9, the flow is similar to that of Case5 after the 3rd row of pin-fins, as found in

Fig. 6(d)(h) and Fig. 7(d)(h). Therefore, the influence of the jet effect on the flow field is mainly in zone of the first three rows of pin-fins.

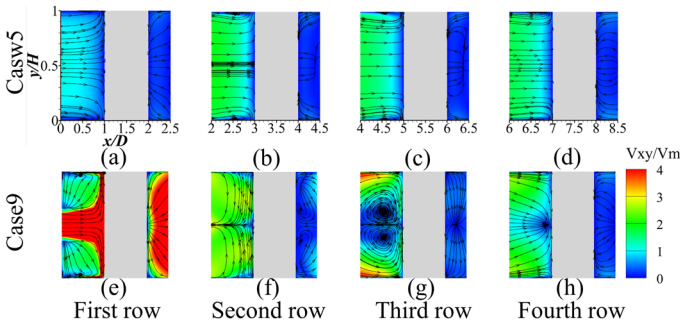

Fig. 7 Flow field characteristics on the central longitudinal section before and after the pin-fins of each row, Re_{Dh}=6000

Heat transfer

Fig. 8 shows the temperature contours on the heated wall for cases 2-9. One can also find that the jet impingement provides better cooling of the pin-fins channel compared to the uniform inlet cases, especially in the zone before the leading edge of 3rd row of pin-fins, due to the aforementioned flow field characteristics. To further quantitatively understand the heat transfer enhancement of the channel around each row of pin-fins by jet impingement, taking Case5 and Case9 as examples, the varies of average Nusselt number on the heated wall around each pin-fins row ($\overline{Nu}_{pin}$) with Reynolds number of channel (Re_{Dh}) are shown in Fig. 9. It can be seen that $\overline{Nu}_{pin}$ around the first two pin-fins rows under the jet flow condition of Case9 is 2-3 times higher than that of the uniform flow condition of Case5 under the same Re_{Dh}. $\overline{Nu}_{pin}$ decreases in pin-fins rows for jet flow case. And $\overline{Nu}_{pin}$ of the jet flow is almost the same as the uniform flow around the 4th row of pin-fins. What's more, $\overline{Nu}_{pin}$ basically increases with the increase of Re_{Dh}. Fig. 10 shows that the number of pin-fins rows in the channel has little effect on $\overline{Nu}_{pin}$. Therefore, for the cooling structure of pin-fins channel with jet flow, the number of pin-fins rows can be appropriately decreased to obtain the optimal heat transfer enhancement in the internal cooling of turbine blade's trailing edge with the small internal space.

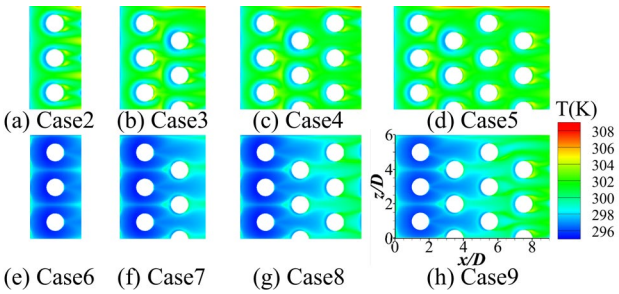

Fig. 8 Temperature contour at the bottom heated wall in pin-fins channel,Re_{Dh} = 6000

Friction Factor

Again, taking Case 5 and Case 9 as examples, the variations of the friction factors with flow distance are shown in Fig. 11. It can be seen that the friction factor increases sharply through jet holes of the perforated plate in the jet flow case, in which the flow resistance through the pin-fins arrays is neglectable. While in the uniform flow case the friction factor increases in pin-fins rows. The friction factor of Case9 is almost 100 times higher than that of Case5 because of too small cross sectional area ration of jet holes to channel in our present work. This means the effect of cross-sectional area ration of jet holes to channel on the overall performance pin-fins channel cooling is significant. The checking of this area ratio effect is our next work.

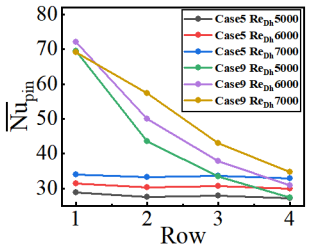

Fig. 9 $\overline{Nu}_{pin}$ under different Re_{Dh}

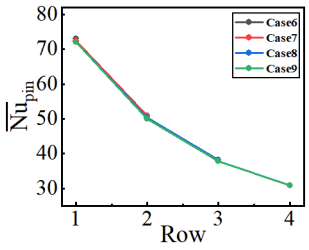

Fig. 10 $\overline{Nu}_{pin}$ for cases of 6-9, Re_{Dh}= 6000

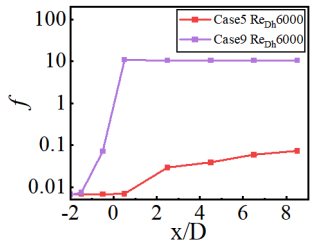

Fig. 11 Friction factor for Case5 and Case9

4.2. Effect of jet holes arrangement on the flow and heat transfer in a four-row pin-fins array channel

Flow field

In this section, the results of cases 10-13 are presented and compared to that of Case9. Fig. 12 and Fig. 13 show the flow structure of Case10, 11, 12 and 13. By comparing the Fig. 7(f) and Fig. 13(a), the velocity of the secondary impact flow of Case10 is much faster than Case9. In the Case11, the velocity of the jet decreases significantly when it impacts on second pin-fins row after a long period of bloated development. This results in a reduction of the secondary impact flow velocity, as shown in Fig. 14(c). In addition, the jet is deflected towards the central *xy*-plane due to the long distance from the jet hole to the second row. This phenomenon, referred to as jet curvature in [16], leads to a large amount of air being directed towards the sidewall of the channel, resulting in the formation of a high-velocity zone in the upper left corner, as shown in Fig. 12(b) and (f).

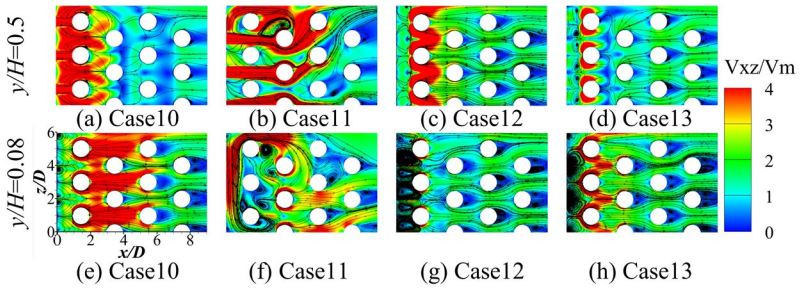

Fig. 12 Flow structure in the pin-fins channel with different jet hole arrangements， Re_{Dh}=6000

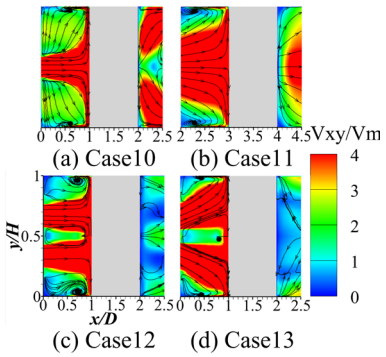

Fig. 13 Flow field characteristics on the central longitudinal section before and after the pin-fins of each row, Re_{Dh}=6000

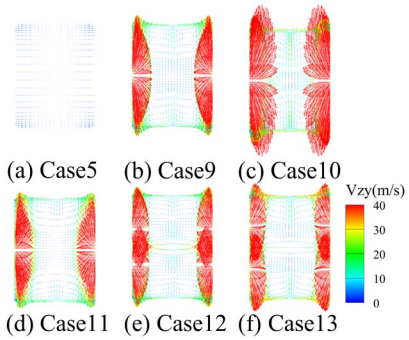

Fig. 14 Velocity vector between two pin-fins which row is impacted by the jet directly， Re_{Dh}=6000

For the Case12 and Case13, a large portion of the secondary impact flow is directed towards the central *xz*-plane, as shown in Fig. 13(c)(d) and Fig. 14(e)(f). The secondary impact flows with opposite directions converge in this plane, resulting in a large momentum loss and reduced airflow to the heated wall. The high-velocity region near the heated wall is almost exclusively located at the leading edge of the first row of pin-fins. Owing to the reduced air momentum, the flow structure in the channel approaches a uniform flow more quickly, and the effect of the jet is almost negligible beneath the 2nd row of pin-fins. In Case13, the inclined double-layered jet holes result in less momentum consumption

in the central *xz*-plane compared to Case12, as shown in Fig. 13(d) and Fig. 14(f).

Heat transfer

Fig. 15 shows the temperature contours on the heated wall for cases 10-13. The large low-temperature area of Case10 is still maintained in the first three rows of pin-fins and is larger in extent and lower in temperature than Case9. For Case 11, the area of lowest temperature occurs at the second row of pin-fins, consistent with the flow field characteristics shown in Fig. 12(f). In Fig. 16, the $\overline{Nu}_{pin}$ of Case10 is higher than that of Case 9. This indicates that an arrangement of jet holes with smaller area ratios is more favorable for enhancing the heat transfer intensity in the pin-fin channel. For Case11, the position of the jet impinging on the pin-fins is shifted back to the second row. Consequently, the effect of the jet on heat transfer in the pin-fin channel is also shifted accordingly, as shown in Fig. 16. Additionally, for Case 12, the $\overline{Nu}_{pin}$ at the last two rows is smaller than the Case5 and is also smaller than that of Case 9 at the first row. The $\overline{Nu}_{pin}$ of Case 13 is higher than that of Case 12 and exceeds that of Case 9 at the first row. This is attributed to the jet being closer to the heated wall and the secondary impact flow impinging on the heated wall having a greater velocity, which compensates for the reduced airflow. Consequently, the adverse effects of the double-layer structure can be mitigated by increasing the tilt angle of the jet holes.

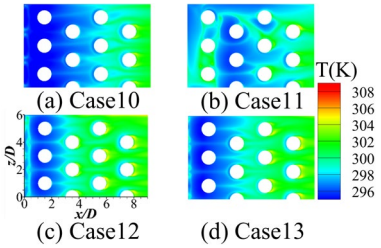

Fig. 15 Temperature contour at the bottom heated wall with different jet hole arrangements， Re_{Dh}=6000

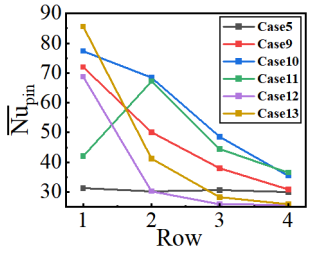

Fig. 16 $\overline{Nu}_{pin}$ for different cases， Re_{Dh}=6000

Friction factor

From Fig. 17, the high-pressure area occurs at all locations where the jet directly impacts the pin-fins. The low-pressure region in Case 11 extends to the second row of pin-fins, indicating that the extent of the low-pressure region is related to the initial impingement location of the jet on the pin-fins. Cases 9, 11, 12, and 13 exhibit similar friction factors, whereas Case 10 has a friction factor approximately five times larger than those of the other cases, as illustrated in Fig. 18. Therefore, although a smaller jet holes area is beneficial for enhancing heat transfer, it also leads to a significant increase in friction loss.

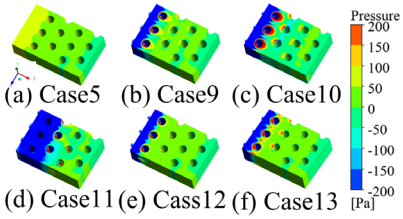

Fig. 17 Pressure contour for different cases， Re_{Dh}=6000

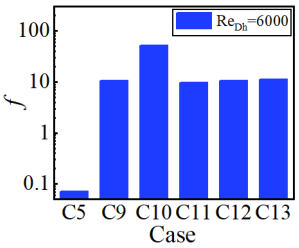

Fig. 18 Friction factor for different cases

5. Conclusions

(1) The effect of the jet on the flow field and heat transfer in the pin-fin channel is primarily concentrated in the first three rows of pin-fins. The Nusselt number for the heated wall beneath the first two rows is 2-3 times higher than that of uniform flow conditions. However, the friction factor in the channel is 100 times greater. At the fourth row of pin-fins, the flow structure and Nusselt number closely resemble those of the uniform flow case.

(2) Among five different jet holes arrangements on the perforated plate, a smaller area ratio of jet holes to the channel cross-section shows the best heat transfer performance. However, the friction factor increases dramatically as the area ratio decreases. What's more, a staggered-jet-holes arrangement results in a backward displacement of both the jet's effective zone and the heat transfer enhancement zone.

(3) In this research, the area of the jet hole has the most significant impact on heat transfer in the pin-fin channel. To achieve a more optimal arrangement, further design optimization of the jet holes is necessary.

Acknowledgements

The work presented in this paper is supported by the National Science and Technology Major Project (J2019-III-0007-0050).

References

[1] S. C. Gülen and M. Curtis, "Gas turbine's role in energy transition," *Journal of Engineering for Gas Turbines and Power,* vol. 146, no. 10, pp. 101008, 2024.

[2] G. J. Vanfossen, "Heat-transfer coefficients for staggered arrays of short pin fins," *J. Eng. Power-Trans. ASME,* vol. 104, no. 2, pp. 268-274, 1982.

[3] D. E. Metzger, C. S. Fan and S. W. Haley, "Effects of pin shape and array orientation on heat transfer and pressure loss in pin fin arrays," *Asme Transactions Journal of Engineering Gas Turbines & Power,* vol. 106, no. 1, pp. 252-257, 1984.

[4] K. K. Ferster, K. L. Kirsch and K. A. Thole, "Effects of geometry, spacing, and number of pin fins in additively manufactured microchannel pin fin arrays," *J. Turbomach.-Trans. ASME,* vol. 140, no. 1, pp. 011007, 2018.

[5] L. Huang, Q. L. Li and H. Y. Zhai, "Experimental study of heat transfer performance of a tube with different shaped pin fins," *Appl. Therm. Eng.,* vol. 129, pp. 1325-1332, 2018.

[6] J. Xu, J. X. Yao, P. F. Su, J. Lei, J. M. Wu and T. Y. Gao, "Heat transfer and pressure loss characteristics of pin-fins with different shapes in a wide channel," in *ASME Turbo Expo: Turbine Technical Conference and Exposition*, Charlotte, NC, 2017, vol. 5A: Heat Transfer, pp. 106684.

[7] W. Jin, J. M. Wu, N. Jia, J. Lei, W. T. Ji and G. N. Xie, "Effect of shape and distribution of pin-fins on the flow and heat transfer characteristics in the rectangular cooling channel," *Int. J. Therm. Sci.,* vol. 161, pp. 106758, 2021.

[8] M. Axtmann, R. Poser, J. von Wolfersdorf and M. Bouchez, "Endwall heat transfer and pressure loss measurements in staggered arrays of adiabatic pin fins," *Appl. Therm. Eng.,* vol. 103, no. 103, pp. 1048-1056, 2016.

[9] H. S. Ahn, S. W. Lee, S. C. Lau and D. Banerjee, "Mass (heat) transfer downstream of blockages with round and elongated holes in a rectangular channel," *J. Heat Transf.-Trans. ASME,* vol. 129, no. 12, pp. 1676-1685, 2007.

[10] H. Chung, J. S. Park, H. S. Sohn, D. H. Rhee and H. H. Cho, "Trailing edge cooling of a gas turbine blade with perforated blockages with inclined holes," *Int. J. Heat Mass Transf.,* vol. 73, pp. 9-20, 2014.

[11] S. C. Lau, J. Cervantes, J. C. Han, R. J. Rudolph and K. Flannery, "Measurements of wall heat (mass) transfer for flow through blockages with round and square holes in a wide rectangular channel," *Int. J. Heat Mass Transf.,* vol. 46, no. 21, pp. 3991-4001, 2003.

[12] S. Shin and J. S. Kwak, "Effect of hole shape on the heat transfer in a rectangular duct with perforated blockage walls," *Journal of Mechanical Science & Technology,* vol. 22, no. 10, pp. 1945-1951, 2008.

[13] S. Schekman, M. D. Atkins and T. Kim, "Local end-wall heat transfer enhancement by jet impingement on a short pin-fin," *Int. J. Heat Mass Transf.,* vol. 128, pp. 1033-1047, 2019.

[14] R. Kan, J. Ren and H. D. Jiang, "Combined effects of perforated blockages and pin fins in a trailing edge internal cooling duct," in *ASME Turbo Expo: Turbine Technical Conference and Exposition*, Dusseldorf, GERMANY, 2014, vol. 5A: Heat Transfer, pp. 111006.

[15] S. Peng, W. Jin and J. Wu, "Effects of heat load and inlet flow conditions on heat transfer in channels with pin fin arrays," *Journal of Propulsion Technology,* vol. 43, no. 8, pp. 298-308, 2022.

[16] S. Schekman and T. Kim, "Orifice jet curvature and its interaction with a row of short pin-fins," *J. Fluids Eng.-Trans. ASME,* vol. 146, no. 5, pp. 051302, 2024.